



---

# **NRC - CNRC**

---

## **Grid Optimization for the Full-Scale Test Facility to Evaluate the Fire Performance of Houses – Part 1 – Basement Fires**

**Bounagui, A.; Bénichou, N.; McCartney, C.;  
Kashef, A.**

**IRC-RR-149**

**February 2004**

<http://irc.nrc-cnrc.gc.ca/ircpubs>



National Research  
Council Canada

Conseil national  
de recherches Canada

---

# **NRC - CNRC**

---

## **Grid Optimization for the Full-scale test facility to evaluate the Fire Performance of Houses - Part I- Basement Fires**

Research Report 149

**Date:** 10 February, 2004

**Authors:**

Abderrazzaq Bounagui

Noureddine Bénichou

Cameron McCartney

Ahmed Kashef

Published by  
Institute for Research in Construction  
National Research Council Canada  
Ottawa, Canada  
K1A 0R



## ABSTRACT

In the event of a house fire, the occupants may be harmed by the untenable conditions that may develop during the fire. The time to untenable conditions can be estimated using experimental studies or numerical simulations. Experimental studies usually provide realistic information but are expensive and time consuming. Numerical simulations, using validated models, can therefore be used to overcome these drawbacks and may also be used to help in the design of experiments.

As part of a research project to evaluate life safety in houses, the Fire Risk Management Program at IRC/NRC has carried out numerical simulations to study the fire performance of houses. The numerical simulations were conducted using the Fire Dynamics Simulator (FDS)<sup>1</sup>, a CFD model developed by the US. National Institute of Standards and Technology (NIST). As a first step, the effect of the CFD grid sizes on the simulation results of the house fire was investigated in order to determine an optimum grid size that could be adopted for future simulations. Several fire sizes were investigated and the optimum grid resolution was found. The chosen grid resolution was then used to determine the time when conditions would become untenable, based on existing criteria from the literature.

This report presents the details of the grid resolution analysis study as well as an evaluation of life safety in houses.

## TABLE OF CONTENTS

<b>ABSTRACT</b> .....	<b>I</b>
<b>TABLE OF CONTENTS</b> .....	<b>II</b>
<b>LIST OF TABLES</b> .....	<b>IV</b>
<b>LIST OF FIGURES</b> .....	<b>V</b>
<b>NOMENCLATURE</b> .....	<b>VI</b>
<b>1 INTRODUCTION</b> .....	<b>1</b>
<b>1.1 CFD Fire Model</b> .....	<b>1</b>
<b>1.2 Model set-up and boundary conditions</b> .....	<b>1</b>
1.2.1 Geometry .....	1
1.2.2 Vents .....	2
1.2.3 Material properties .....	2
1.2.4 Boundary Conditions.....	2
1.2.5 Fire specification .....	3
1.2.6 Position of the thermocouple.....	3
<b>2 GRID RESOLUTION ANALYSIS</b> .....	<b>6</b>
<b>2.1 Resolution Criteria</b> .....	<b>6</b>
<b>2.2 Tenability criteria</b> .....	<b>7</b>
<b>2.3 Fire 1- 1500 kW</b> .....	<b>7</b>
2.3.1 Temperature predictions .....	8
2.3.2 CO prediction .....	10
2.3.3 Basement CO <sub>2</sub> prediction.....	11
2.3.4 Extinction coefficient prediction .....	13
2.3.5 Predictions of the centreline temperature of the fire .....	14
<b>2.4 Fire 2- 2500 kW</b> .....	<b>17</b>
2.4.1 Temperature prediction .....	17
2.4.2 CO prediction .....	19
2.4.3 CO <sub>2</sub> prediction.....	20
2.4.4 Extinction coefficient prediction .....	22

<b>2.5</b>	<b>Fire 3- 3000 kW .....</b>	<b>24</b>
2.5.1	Temperature prediction .....	24
2.5.2	CO prediction .....	27
2.5.3	CO <sub>2</sub> prediction.....	27
2.5.4	Extinction coefficient prediction .....	28
<b>CONCLUSION.....</b>		<b>29</b>
<b>REFERENCES .....</b>		<b>30</b>

## LIST OF TABLES

Table 1: Thermal Properties .....	2
Table 2: Time to peak values for the three fires.....	3
Table 3: Thermocouple trees in the basement.....	4
Table 4: Thermocouple trees on the ground floor .....	4
Table 5: Thermocouple trees up the centre of the stair openings .....	4
Table 6: CO measurements .....	5
Table 7: CO <sub>2</sub> measurements .....	5
Table 8: Extinction Coefficient measurements .....	5
Table 9: Thermocouple at the centreline of the fire .....	5
Table 10 Grid sizes for the basement domain.....	6
Table 11: Tenability criteria .....	7
Table 12: Fire 1: $\dot{Q}$ =1500 kW and $D^*$ =1.13 m.....	7
Table 13: Plume centreline temperature comparisons .....	15
Table 14: Fire 2: $\dot{Q}$ =2500 kW and $D^*$ =1.38 m.....	17
Table 15: Fire 3: $\dot{Q}$ =3000 kW and $D^*$ =1.49 m.....	24

**LIST OF FIGURES**

Figure 1: Perspective view of the Facility.....2

Figure 2: Computation time for all cases.....8

Figure 3: Time-temperature profiles for 0.1 m below basement ceiling- SWQP .....9

Figure 4: Time-temperature profiles 0.1 m below basement ceiling- NWQP .....9

Figure 5: Time-temperature profiles 0.1 m below basement ceiling- NEQP ..... 10

Figure 6: CO measurements at height 1.5 m – SWQP ..... 10

Figure 7: CO measurements at height 1.5 m – NWQP ..... 11

Figure 8: CO measurements at height 1.5 m – NEQP ..... 11

Figure 9: CO<sub>2</sub> concentration at height 1.5 m – SWQP ..... 12

Figure 10: CO<sub>2</sub> concentration at height 1.5 m- NWQP ..... 12

Figure 11: CO<sub>2</sub> concentration at height 1.5 m- NEQP ..... 13

Figure 12: Extinction coefficient at height 1.5 m- SWQP..... 13

Figure 13: Extinction coefficient at height 1.5 m - NWQP ..... 14

Figure 14: Extinction coefficient at height 1.5 m - NEQP ..... 14

Figure 15: Temperature at various heights in the fire plume at 239 s ..... 15

Figure 16: Comparisons of FDS Prediction of the ceiling jet temperature with  
Alpert correlation..... 16

Figure 17: Time-temperature profiles 0.1 m below basement ceiling- SWQP ..... 17

Figure 18: Time-temperature profiles 0.1 m below basement ceiling - NWQP ..... 18

Figure 19: Time-temperature profiles 0.1 m below basement ceiling – NEQP ..... 18

Figure 20: Comparison of FDS Predictions of ceiling jet temperature with Alpert  
correlation..... 19

Figure 21: CO concentration at height 1.5 m- SWQP ..... 19

Figure 22: CO concentration at height 1.5 m - NWQP ..... 20

Figure 23: CO concentration at height 1.5 m - NEQP ..... 20

Figure 24: CO<sub>2</sub> concentration at height 1.5 m - SWQP ..... 21

Figure 25: CO<sub>2</sub> concentration at height 1.5 m - NWQP ..... 21

Figure 26: CO<sub>2</sub> concentration at height 1.5 m - NEQP ..... 22

Figure 27: Extinction coefficient at height 1.5 m - SWQP ..... 22

Figure 28: Extinction coefficient at height 1.5 m - NWQP ..... 23

Figure 29: Extinction coefficient at height 1.5 m N° 54- NEQP ..... 23

Figure 30: Time- temperature profiles for thermocouple N° 2- SWQP ..... 25

Figure 31: Time-temperature profiles for thermocouple N° 12- NWQP ..... 25

Figure 32: Time- temperature profiles for thermocouple N° 17- NEQP ..... 26

Figure 33: Comparisons of FDS prediction of the ceiling jet temperature with  
Alpert correlation..... 26

Figure 34: CO concentration at three points of the basement at height 1.5 m ..... 27

Figure 35: CO<sub>2</sub> concentration at three points of the basement at height 1.5 m ..... 28

Figure 36: Extinction coefficient at three points of the basement at height 1.5 m ..... 28



## NOMENCLATURE

- $D^*$  : characteristic fire diameter, m;  
 $D$  : effective diameter, m;  
 $\dot{Q}$  : total heat release rate, kW;  
 $\rho_\infty$  : density at ambient temperature, kg/m<sup>3</sup>;  
 $c_p$  : specific heat of gas, kJ/kg.K;  
 $T_\infty$  : ambient temperature, K;  
 $g$  : acceleration of gravity, m/s<sup>2</sup>;  
 $\delta x$  : grid size in x direction, m;  
 $\delta y$  : grid size in y direction, m;  
 $\delta z$  : grid size in z direction, m;  
 $T_{pl}$  : plume gas temperature, °C;  
 $K$  : configuration parameter;  
 $H$  : vertical distance above fire, m;  
 $R$  : radial distance from the centreline of the plume, m;  
 $Q$  : heat release rate of the fire, kW.

## **1 Introduction**

In order to evaluate life safety in houses, the Fire Risk Management program at IRC/NRC, has carried out numerical simulations in preparation for a study of fires in houses. The numerical simulations were conducted using Fire Dynamics Simulator (FDS)<sup>1</sup>. The effect of the grid sizes on the simulation results of a fire in a house was investigated in order to determine an optimum grid size that will be adopted for future simulations.

The Computational Fluid Dynamics (CFD) numerical simulations are computationally very expensive. One of the most significant factors influencing the computation time is the size of the computational grid specified by the user. Because it is possible to over-resolve or under-resolve a space by specifying grids that are too fine or too coarse, it is important to determine an appropriate grid size that would optimize the solution accuracy and time.

This report presents the details of the grid sensitivity analysis that was performed based on the full-scale facility constructed at the NRC laboratory to investigate the fire performance of houses. Three different basement fire sizes were modelled. Further investigation on the grid sizes will be performed when the full-scale test data will be available.

### **1.1 CFD Fire Model**

FDS is a Computational Fluid Dynamics (CFD) fire model that employs the large eddy simulation (LES) techniques<sup>1</sup> to compute gas density, velocity, temperature, pressure and species concentrations in each control volume. FDS has been demonstrated to predict thermal conditions resulting from a fire in an enclosure<sup>1,2</sup>. A complete description of the FDS model is given in reference<sup>1</sup>.

### **1.2 Model set-up and boundary conditions**

FDS requires as inputs: geometry of the domain being modelled, computational cell size, location of the ignition source, fuel type, heat release rate, material thermal properties of obstructions, vents location and boundary conditions.

#### **1.2.1 Geometry**

The full-scale test facility is a three-storey building. Figure 1 shows a perspective view of the facility. The three levels of the facility are enclosed within a 10.8 m x 9.2 m x 8.2 m tall rectangular volume.

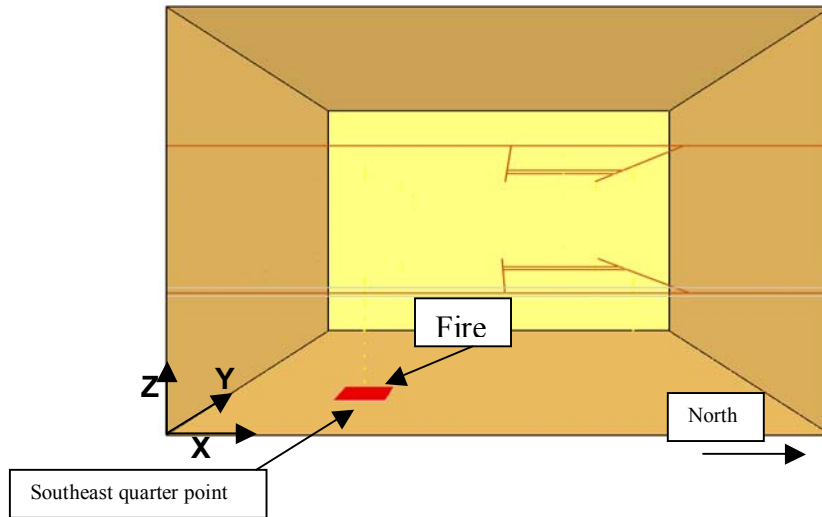


**Figure 1: Perspective view of the Facility**

### 1.2.2 Vents

This simulation considered the following openings:

- Opening to the outside of the structure is located in the main floor of the facility and is approximately 0.9 m wide x 2.4 high.
- First stairway opening from the basement to the main floors which is approximately 3 m x 0.9 m at a height of 2.7 m.
- Second stairway opening from the main floor to the second floor which is approximately 3 m x 0.9 m at a height of 5.48 m.

These vents were assumed to be open during the entire simulation.

### 1.2.3 Material properties

The ceilings and floors of the facility are assumed to be composed of steel. The walls are composed of gypsum board. The input data given in Table 1 is taken from the database provided by FDS.

STEEL		GYPSUM BOARD		
Specific heat x density x thickness (KJ/K.m <sup>2</sup> )	Thickness (m)	Conductivity (W/m K)	Diffusivity (m <sup>2</sup> /s)	Thickness (m)
20	0.005	0.48	4.1E-7 10 <sup>-7</sup>	0.013

**Table 1: Thermal Properties**

### 1.2.4 Boundary Conditions

The floor and the ceiling are considered thermally-thin walls: i.e. the temperature is assumed to be the same throughout their width.

### 1.2.5 Fire specification

Three fire sizes were considered in this study with peaks ranging from 1500 to 3000 kW (see Table 2). These fires start at  $t=0$  of the simulation and grow according to a fast t-squared curve ( $\alpha = 0.0469 \text{ kW/s}^2$ ) to a constant peak value. The fire source was approximated as a rectangular object representing a propane burner with a specified heat release rate. The fire area of the propane burner is 1.0 m wide by 1.0 m long located on the floor of the basement. The time to peak values of the three fires are summarized in Table 2. The heat release will remain constant after the time to peak value.

$Q_{peak} \text{ (kW)}$	$t_{peak} \text{ (s)}$
1500	179
2500	231
3000	253

**Table 2: Time to peak values for the three fires**

### 1.2.6 Position of the thermocouple

In the model, the thermocouple trees, as well as the measurement of CO, CO<sub>2</sub> and the extinction coefficient, are placed at different points in the basement to record the predicted quantities. Table 3 to Table 9 shows the positions of the measurements that were recorded.

	Thermocouple Number	Position (m)		
		X	Y	Z
South West quarter point (SWQP)	1	2.69	6.93	2.69
	2	2.69	6.93	2.64
	3	2.69	6.93	2.54
	4	2.69	6.93	2.44
	5	2.69	6.93	2.24
South East quarter point (SEQP)	6	2.69	2.31	2.69
	7	2.69	2.31	2.64
	8	2.69	2.31	2.54
	9	2.69	2.31	2.44
	10	2.69	2.31	2.24
North West quarter point (NWQP)	11	8.08	6.93	2.69
	12	8.08	6.93	2.64
	13	8.08	6.93	2.54
	14	8.08	6.93	2.44
	15	8.08	6.93	2.24

North East quarter point (NEQP)	16	8.08	2.31	2.69
	17	8.08	2.31	2.64
	18	8.08	2.31	2.54
	19	8.08	2.31	2.44
	20	8.08	2.31	2.24

**Table 3: Thermocouple trees in the basement**

	Thermocouple Number	Position (m)		
		X	Y	Z
South West quarter	21	2.69	6.93	5.38
	22	2.69	6.93	5.28
	23	2.69	6.93	5.18
	24	2.69	6.93	5.08
South East quarter	25	2.69	2.31	5.38
	26	2.69	2.31	5.28
	27	2.69	2.31	5.18
	28	2.69	2.31	5.08
North West quarter	29	8.08	6.93	5.38
	30	8.08	6.93	5.28
	31	8.08	6.93	5.18
	32	8.08	6.93	5.08
North East quarter	33	8.08	2.31	5.38
	34	8.08	2.31	5.28
	35	8.08	2.31	5.18
	36	8.08	2.31	5.08

**Table 4: Thermocouple trees on the ground floor**

Thermocouple Number	Position (m)		
	X	Y	Z
37	6.99	5.19	3.34
38	6.99	5.19	2.74
39	6.99	5.19	2.10
40	6.99	5.19	6.08
41	6.99	5.19	5.48
42	6.99	5.19	4.88

**Table 5: Thermocouple trees up the centre of the stair openings**

The measurement of CO, CO<sub>2</sub> and the extinction coefficient were taken at a height of 1.5 m. This height was chosen to indicate the possible impact effect on the house occupants.

Measurement Number	Description	Position (m)		
		X	Y	Z
43	CO basement South West	2.69	6.93	1.5
44	CO basement South East	2.69	2.31	1.5
45	CO basement North West	8.08	6.93	1.5
46	CO basement North East	8.08	2.31	1.5

**Table 6: CO measurements**

Measurement Number	Description	Position (m)		
		X	Y	Z
47	CO <sub>2</sub> basement South West	2.69	6.93	1.5
48	CO <sub>2</sub> basement South East	2.69	2.31	1.5
49	CO <sub>2</sub> basement North West	8.08	6.93	1.5
50	CO <sub>2</sub> basement North East	8.08	2.31	1.5

**Table 7: CO<sub>2</sub> measurements**

Measurement Number	Description	Position (m)		
		X	Y	Z
51	Extinction Coefficient basement South West	2.69	6.93	1.5
52	Extinction Coefficient basement South East	2.69	2.31	1.5
53	Extinction Coefficient basement North West	8.08	6.93	1.5
54	Extinction Coefficient basement North East	8.08	2.31	1.5

**Table 8: Extinction Coefficient measurements**

Thermocouple Number	Position (m)		
	X	Y	Z
63	2.69	2.31	0.30
64	2.69	2.31	0.60
65	2.69	2.31	0.90
66	2.69	2.31	1.20
67	2.69	2.31	1.50
68	2.69	2.31	1.80
69	2.69	2.31	2.10
70	2.69	2.31	2.40

**Table 9: Thermocouple at the centreline of the fire**

## 2 Grid resolution analysis

To study the effect of the grid size on the prediction of the temperature and the concentration of the CO<sub>2</sub>, simulations were conducted for different grid and fire sizes. The facility geometric domain is partitioned into two domains. The first domain represents the basement and the second represents the remaining storeys. In the model, the fire occurred in the southeast quarter point of the basement (Figure 1). Table 10 presents the grid sizes used for the basement. For the main and second storey, the domain was idealized using a (0.20x0.20x0.20 m) grid distribution.

Cases	Grid sizes (m)
Case 1	0.20x0.20x0.20
Case 2	0.14x0.14x0.14
Case 3	0.10x0.10x0.10
Case 4	0.08x0.08x0.08

**Table 10 Grid sizes for the basement domain**

The basement domain, being the place of fire origin, was the main focus. The parameters of interest were the temperature, visibility, CO and CO<sub>2</sub> concentrations. These parameters were recorded in different quarter points of the basement.

In the following sections, the results of the simulations for the fine grid sizes and the three fire sizes (Table 2) are presented.

### 2.1 Resolution Criteria

The quality of the resolution depends on both the size of the fire and the size of the grid cells [2]. The characteristic fire diameter  $D^*$  combines the effect of the fire effective diameter and its size, defined as follows:

$$D^* = \left( \frac{\dot{Q}}{\rho_{\infty} c_p T_{\infty} \sqrt{g}} \right)^{\frac{2}{5}} = \left( \frac{\dot{Q}}{\rho_{\infty} c_p T_{\infty} \sqrt{g} D D^2} \right)^{\frac{2}{5}} D$$

where:

$D^*$  : characteristic fire diameter, m;

$D$  : effective diameter, m;

$\dot{Q}$  : total heat release rate, kW;

$\rho_{\infty}$  : density at ambient temperature, kg/m<sup>3</sup>;

$c_p$  : specific heat of gas, kJ/kg.K;

$T_{\infty}$  : ambient temperature, K;

$g$  : acceleration of gravity, m/s<sup>2</sup>.

The ratio  $D^* / \max(\delta x, \delta y, \delta z)$  is an indication of the number of cells in the fire region.

Where:  $\delta x, \delta y, \delta z$  : grid sizes in the three Cartesian directions x, y, and z, in meters.

The higher the ratio, the better the representation of the fire and the better the numerical model predictions. The fire resolution index presents the fraction of the ideal

stoichiometric value of the mixture fraction that is being used in the calculation. It indicates how well resolved the calculations are. When the fire resolution index is equal to 1, the calculation is well resolved.

Another dimensionless parameter that can be used to represent the resolution of the fire plume simulation, is the parameter  $R^*$  defined as <sup>4</sup>:

$$R^* = \frac{\max(\delta x, \delta y, \delta z)}{D^*}$$

## 2.2 Tenability criteria

To evaluate life safety in a house, tenability criteria are needed. The Fire Engineering Design Guide<sup>5</sup> in New Zealand adopted the criteria shown in Table 11.

Tenability type	Tenability limit
Toxicity	CO $\leq$ 1400 ppm CO <sub>2</sub> $\leq$ 0.05 mol/mol
Smoke obscuration	Visibility in the relevant layer should not fall below 2 m. This value corresponds to an optical density of 0.5 m <sup>-1</sup>

**Table 11: Tenability criteria**

There are other life safety criteria such as those in the SFPE Handbook<sup>9</sup>, but the New Zealand criteria are used in the current analysis.

## 2.3 Fire 1- 1500 kW

The fire source was approximated as a rectangular object representing a propane burner with a specified heat release rate. Located in the southeast quarter point of the basement, was a propane burner 1.0 m wide and 1.0 m long. The heat release rate of the burner, with a characteristic fire diameter of 1.13 m was assumed to follow a fast T-squared growth, reaching a peak of approximately 1.5 MW in 179 s.

Table 12 shows the different grid distribution, grid size, dimensionless parameter  $R^*$ , Fire resolution index, and computation time.

Cases	Grid number	Grid size (m)	$R^*$	Fire Resolution index (FRI)	Run time (h)
Case 1	54x45x40	0.20	0.17	0.5	2.7
Case 2	75x65x20	0.14	0.12	0.7	8.9
Case 3	108x90x27	0.10	0.08	0.8	30.6
Case 4	135x120x36	0.08	0.07	1	90.4

**Table 12: Fire 1:  $\dot{Q}$ =1500 kW and  $D^*$  =1.13 m**



Figure 2 shows the computation time for the four cases. As anticipated the computation time is higher for the finer grid.

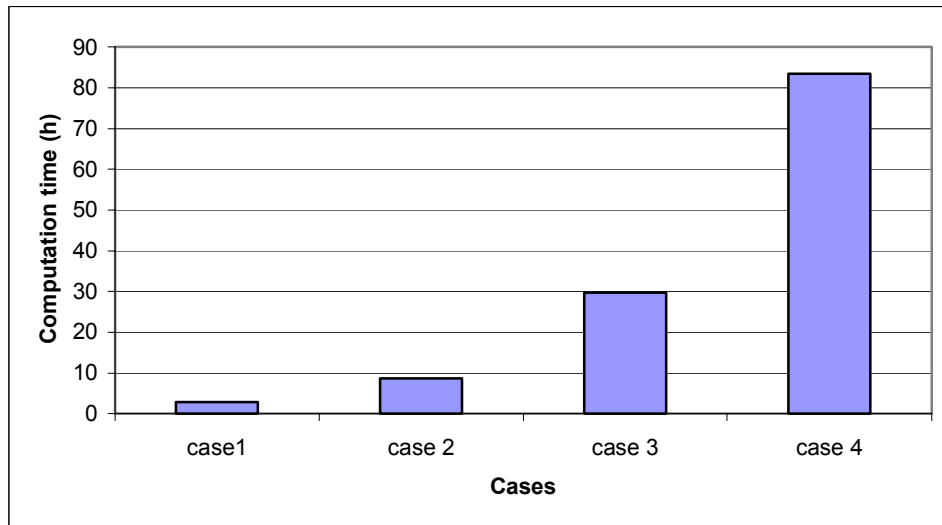


**Figure 2: Computation time for all cases**

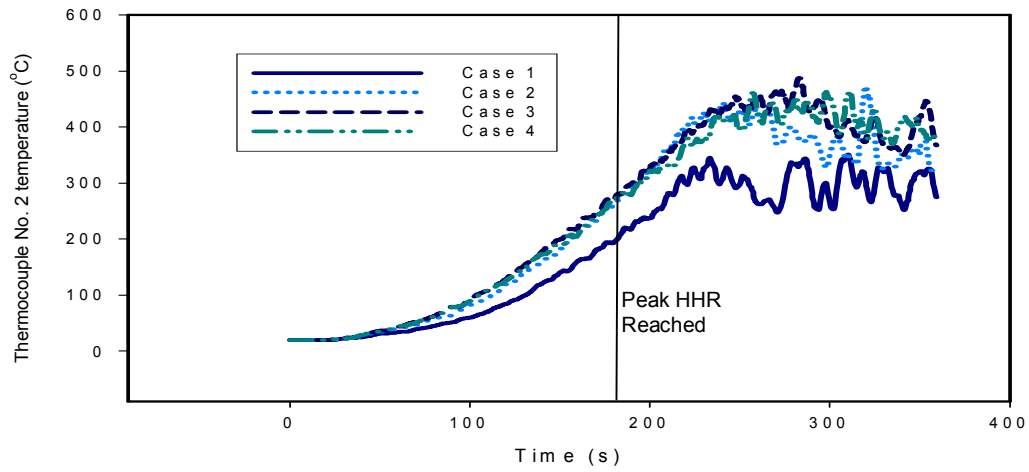
In the following section, the effect of grid sizes on the predictions of gas temperatures, gas concentrations and the extinction coefficient is presented.

### 2.3.1 Temperature predictions

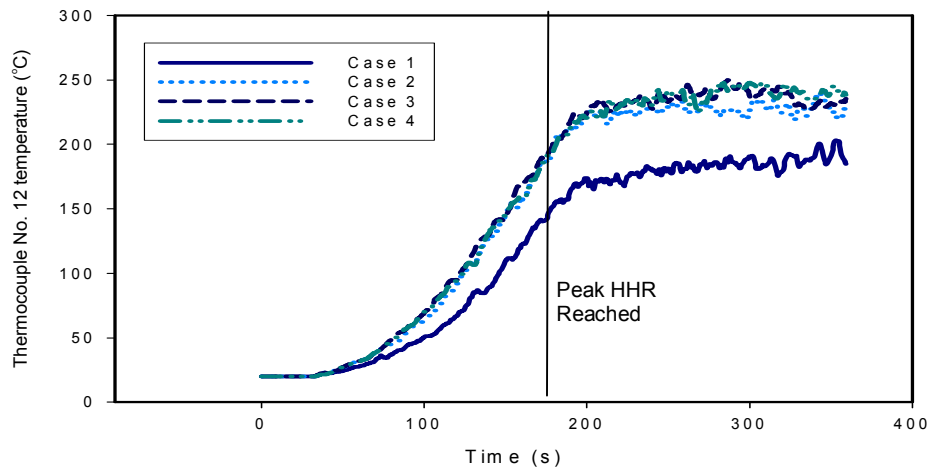
In the model, the thermocouple trees are placed in different quarter points of the basement to record the predicted temperatures. The simulation results from thermocouples N° 2, 12 and 17, located 0.1 m below the basement ceiling in three different points (SWQP, NWQP, NEQP), are presented in this section to highlight the effect of grid size on the estimated temperatures.

Figure 3 to Figure 5 give respectively, the time-temperature profile predictions for thermocouple N° 2, 12 and 17. These figures show similar trends. The predicted temperatures are higher for finer grid sizes.

The computational time is quite high with the finer grid sizes (Figure 2). It is important to find an optimum grid size that resolves the fire well. It is observed that the increase in temperature was limited for  $R^*$  less than 0.08. For Case 4, the fire resolution index is equal to 1 and  $R^*$  is equal to 0.07 (Table 12); thus, the fire is well resolved for Case 4. Therefore, Case 4 will be adopted for this fire.



**Figure 3: Time-temperature profiles for 0.1 m below basement ceiling- SWQP**



**Figure 4: Time-temperature profiles 0.1 m below basement ceiling- NWQP**

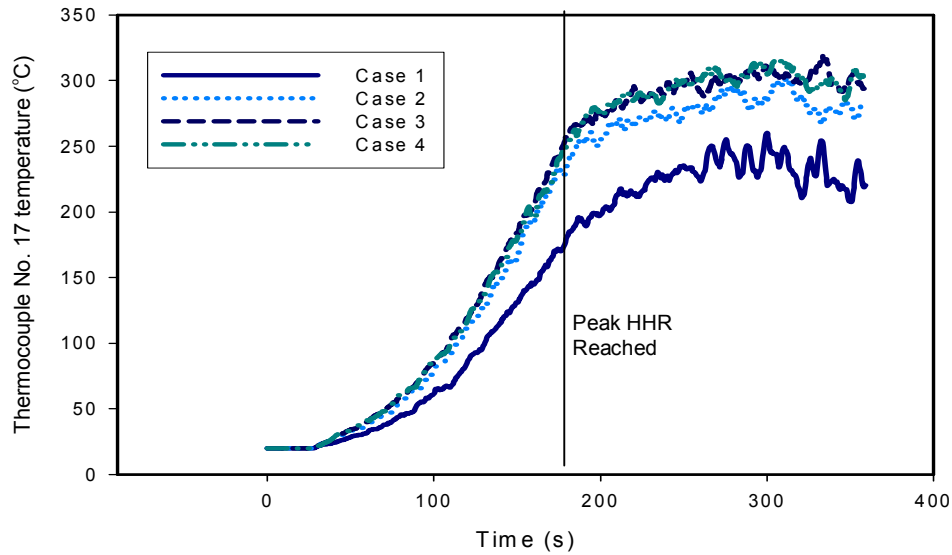


**Figure 5: Time-temperature profiles 0.1 m below basement ceiling- NEQP**

### 2.3.2 CO prediction

Figures 6 through 8 give respectively the CO concentration vs. time for measurements N° 43, 45 and 46 located at 1.5 m from the floor in three quarter points of the basement. The figures show that the effect of the grid is minimal on the prediction of the CO concentrations. The maximum CO concentration observed at this height is approximately 120 ppm which is below the critical tenability limit criteria adopted by the Fire Engineering Design Guide<sup>5</sup> that leads to incapacitation.

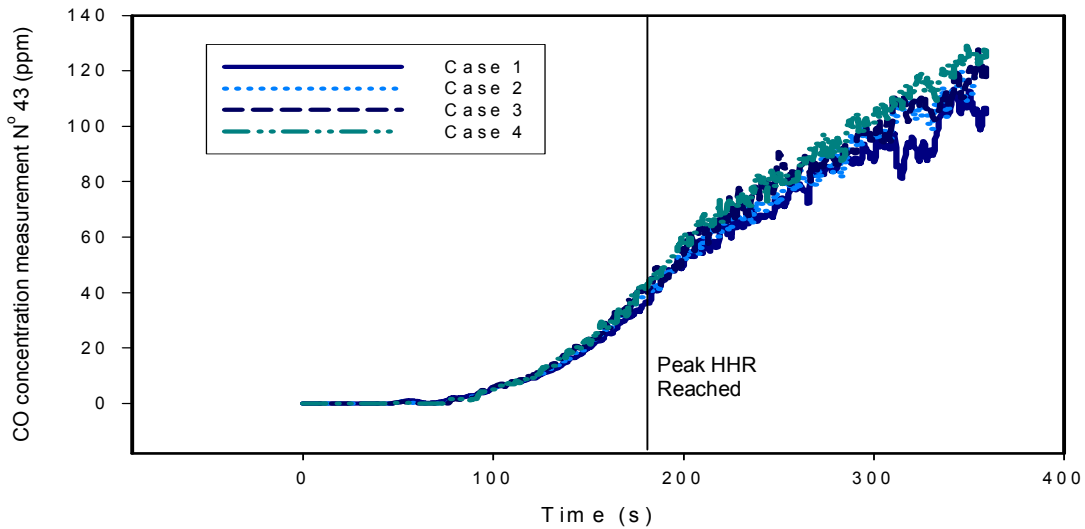


**Figure 6: CO measurements at height 1.5 m – SWQP**

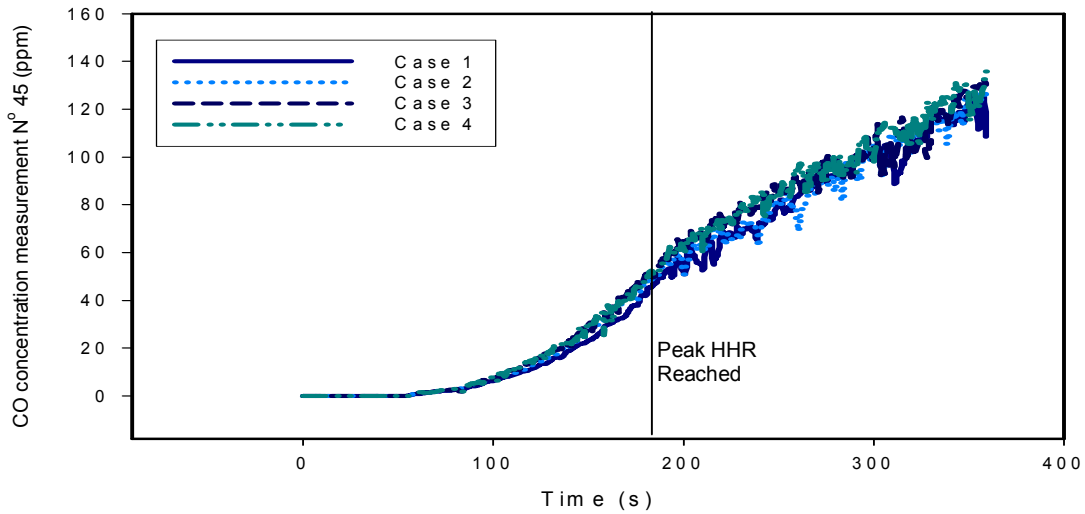


**Figure 7: CO measurements at height 1.5 m – NWQP**

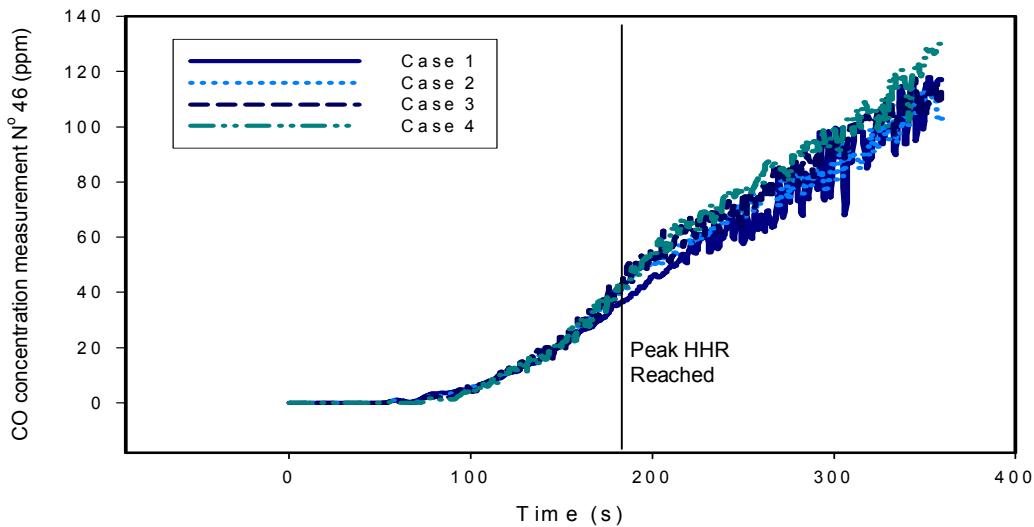


**Figure 8: CO measurements at height 1.5 m – NEQP**

### 2.3.3 Basement CO<sub>2</sub> prediction

Figures 9 through 11 give respectively, the CO<sub>2</sub> concentration vs. time for measurements N°. 47, 49 and 50, located at 1.5 m from the floor in the three quarter point of the basement. The figures show that the effect of the grid is minimal on the prediction of the CO<sub>2</sub> concentration. The maximum CO<sub>2</sub> concentration observed at this height is 0.05 mol/mol. This value can lead to incapacitation based on the tenability limit criteria adopted by the Fire Engineering Design Guide<sup>5</sup> in New Zealand.

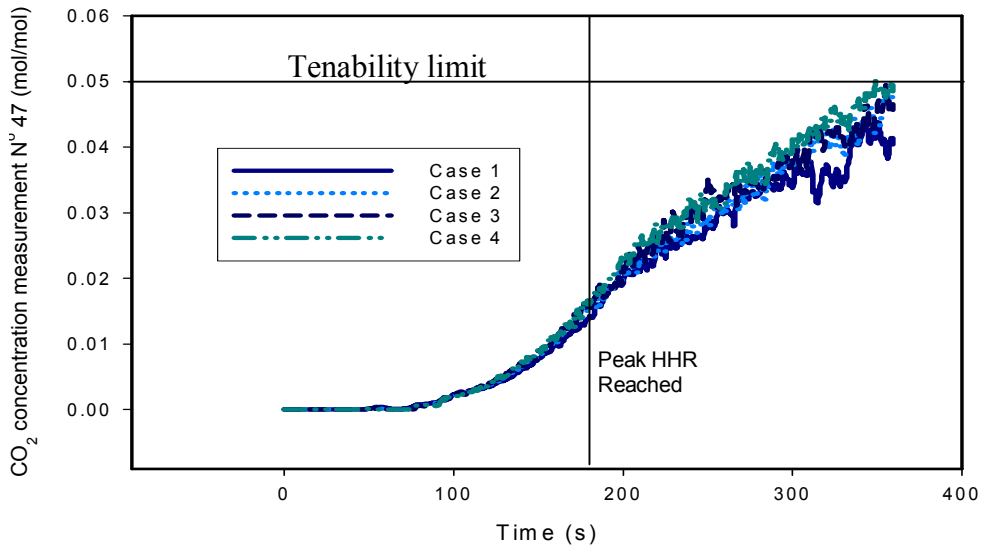


**Figure 9: CO<sub>2</sub> concentration at height 1.5 m – SWQP**

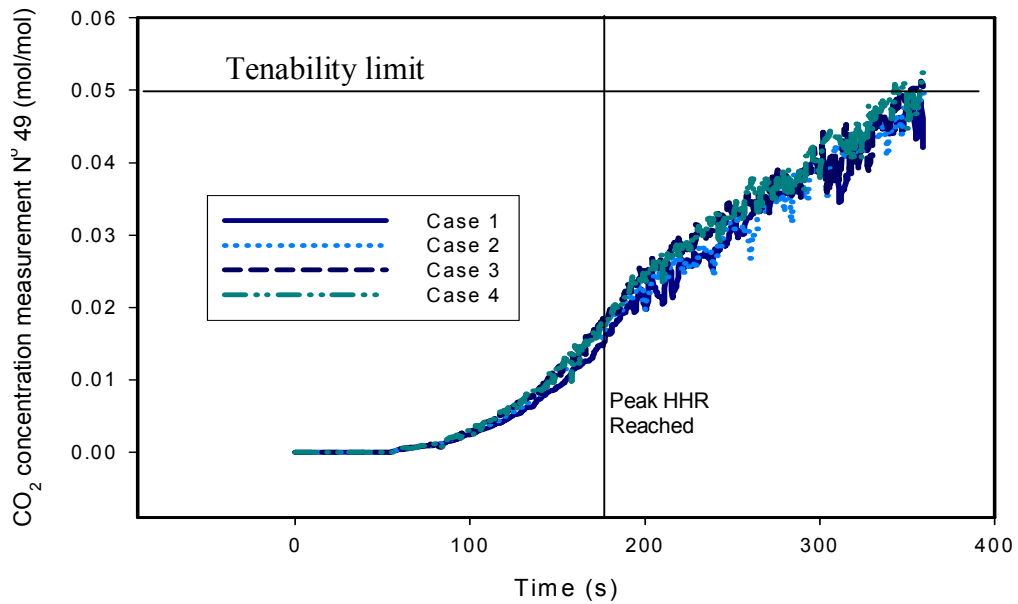


**Figure 10: CO<sub>2</sub> concentration at height 1.5 m- NWQP**

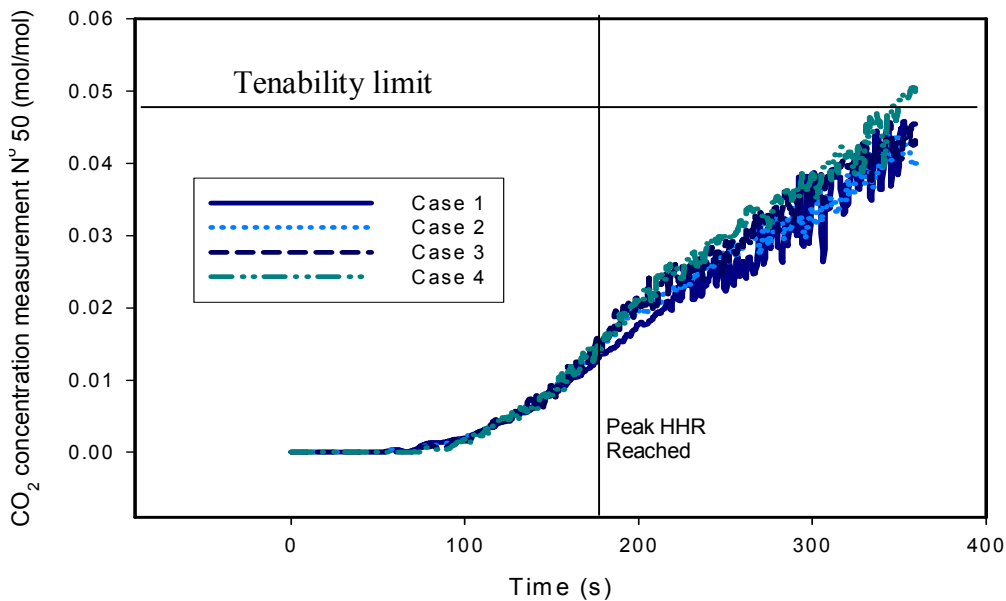


**Figure 11: CO<sub>2</sub> concentration at height 1.5 m- NEQP**

### 2.3.4 Extinction coefficient prediction

Figures 15 through 17 give respectively, the time vs. extinction profile predictions for measurements N° 51, 53 and 54 located at 1.5 m from the floor in three quarter points of the basement. The figures show that the effect of the grid is minimal on the prediction of the extinction coefficient. The maximum of the extinction coefficient observed at this height is approximately 1.6 (1/m) in the tree quarter point. This extinction coefficient value is equal to the optical density as the coefficient relating them is equal to 1. This value should not be higher than 0.5 m<sup>-1</sup> based on the tenability limit criteria<sup>5</sup>. The visibility becomes poor after 180 s.

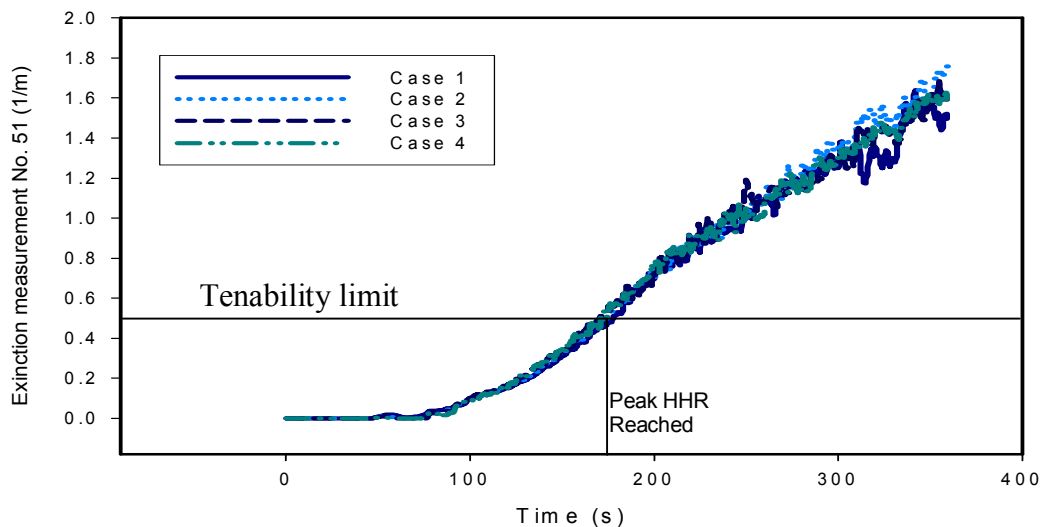


**Figure 12: Extinction coefficient at height 1.5 m- SWQP**

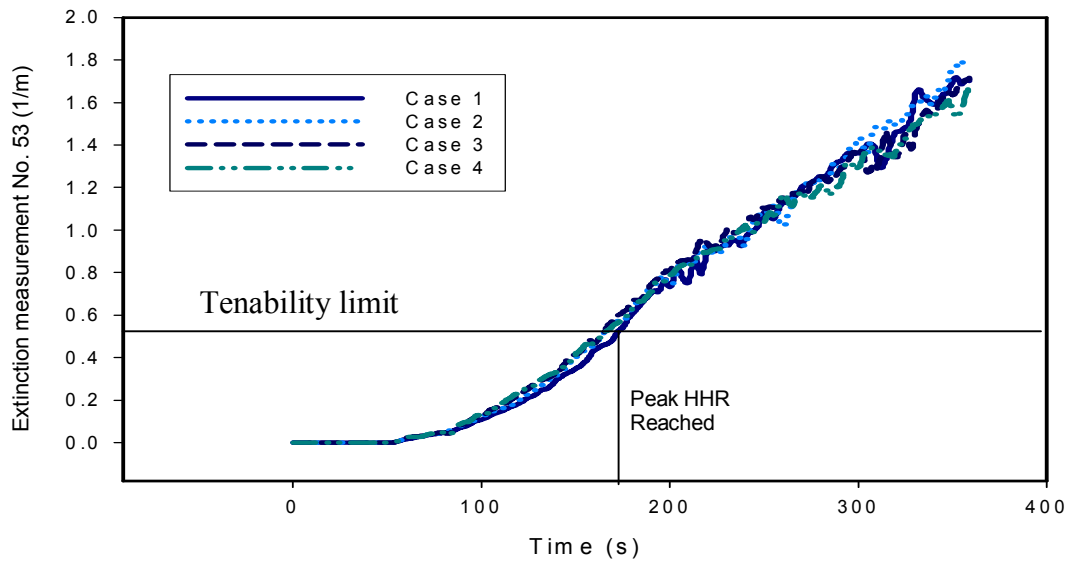


**Figure 13: Extinction coefficient at height 1.5 m - NWQP**

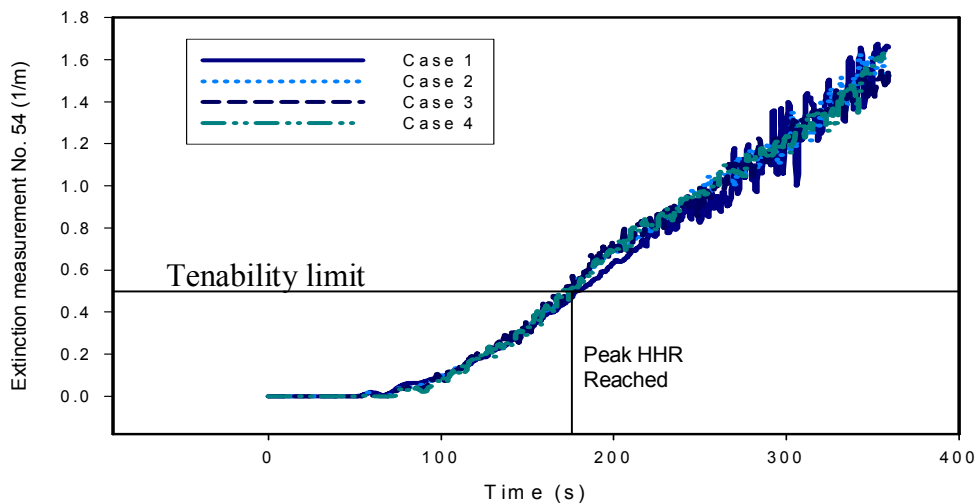


**Figure 14: Extinction coefficient at height 1.5 m - NEQP**

### 2.3.5 Predictions of the centreline temperature of the fire

In the model, a thermocouple tree is placed on the centreline of the fire to record the predicted temperatures of the plume centreline. The locations of the thermocouples are presented in Table 9. The simulation results are presented in this section to highlight the effect of grid size on the estimated temperatures of the centreline of the fire.

FIERASystem Simple Correlation sub-model<sup>6</sup> was used to calculate the plume centreline temperature and to compare it to the CFD predictions. The sub-model uses Heskestad's correlation<sup>7</sup> to determine the plume centreline temperature and is calculated as:

$$T_{cp} = 9.1 \left[ \frac{T_{\infty}}{g \cdot c_p^2 \cdot \rho_{\infty}} \right]^{1/3} Q_c^{2/3} (z - z_0)^{-5/3} + T_{\infty}$$

where:

$T_{cp}$  : plume centreline temperature, K;

$Q_c$  : convective heat release rate, kW;

$z$  : height above top of the fire source, m;

$z_0$  : height of virtual origin relative to the base of fire source, m.

$c_p$  : specific heat of gas, kJ/kg.K

Heskestad estimation	FDS estimation			
	Case 1	Case 2	Case 3	Case 4
839 °C	479 °C	593 °C	962 °C	967 °C

**Table 13: Plume centreline temperature comparisons**

Table 13 shows the values of the temperatures obtained from the Heskestad correlation and FDS prediction for a height of 2.4 m above the fire. The Heskestad correlation provides an estimation that is closer to Cases 3 and 4 of FDS predictions. The finer grids provide better predictions. This means that there is a better characterization of the combustion processes and flame behaviour when the Fire resolution index is close to 1 (Table 12). The coarse grid (Case 1) gives the worse predictions when compared to Heskestad's correlation (Fire resolution index very low (0.2) in Table 12)

Figure 15 shows the temperature profile predictions for the fire plume at various heights. This figure shows a similar trend. The temperature is higher for the finer grid sizes.

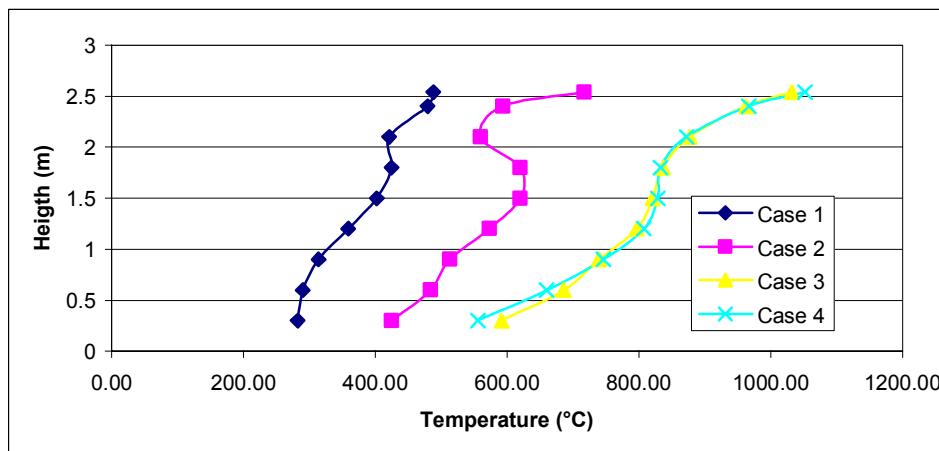


**Figure 15: Temperature at various heights in the fire plume at 239 s**



FIERASystem Simple Correlation sub-model was used to calculate the ceiling jet temperature and to compare it to the CFD predictions. The sub-model uses Alper's correlation<sup>8</sup> to determine the ceiling jet temperature and is defined as:

$$T_{pl} = T_{\infty} + 6.81 \frac{\left( K \cdot \frac{Q}{R} \right)^{2/3}}{H}$$

where:

$T_{pl}$  : plume gas temperature, °C;

$K$  : configuration parameter;

- 1, when the fire is away from any walls;
- 2, when the fire is near a wall;
- 4, when the fire is in a corner;

$H$  : vertical distance above fire, m;

$R$  : radial distance from the centreline of the plume, m;

$Q$  : heat release rate of the fire, kW.

Figure 16 shows the comparison of the predicted temperature at 0.3 m below the basement ceiling with Alper's correlation. Alper's correlation provides an estimation that is closer to Cases 2, 3 and 4 of FDS predictions. The finer grids provide a better prediction (FRI close to 1 in Table 12).

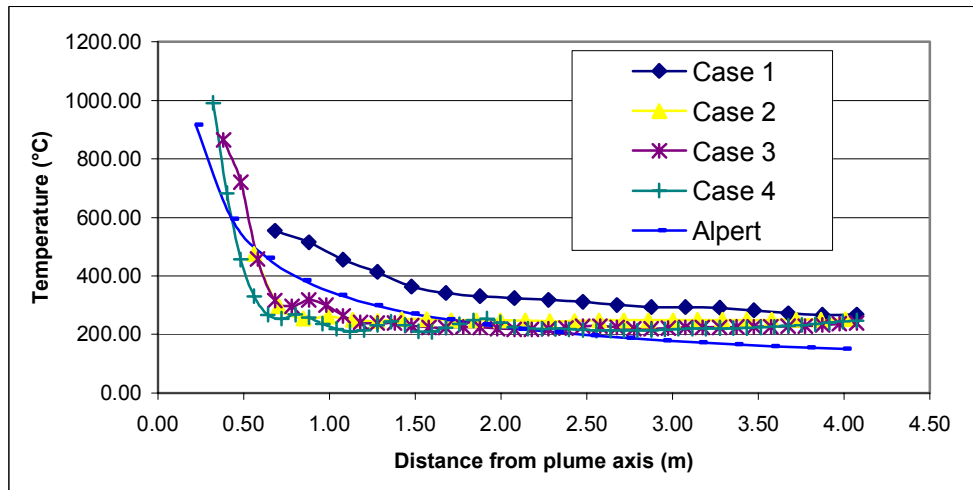


**Figure 16: Comparisons of FDS Prediction of the ceiling jet temperature with Alper's correlation**

## 2.4 Fire 2- 2500 kW

The heat release rate of the fire was assumed to follow a fast T-squared fire, reaching a peak of approximately 2.5 MW in 231s. The characteristic fire diameter is 1.38 m.

Table 14 shows the different cases along with the grid number, grid size, dimensionless parameter  $R^*$ , Fire resolution index, and computation time. The FRI was found to be equal to 1 from the resolution index of 0.07. Thus, the finer grid provides a better prediction.

Cases	Grid number	Grid size (m)	$R^*$	Fire Resolution index (FRI)	Run time (h)
Case 1	54x45x40	0.20	0.14	0.71	2.8
Case 2	75x65x20	0.14	0.1	0.80	8.7
Case 3	108x90x27	0.10	0.07	1	29.7
Case 4	135x120x36	0.08	0.05	1	83.4

Table 14: Fire 2:  $\dot{Q}=2500$  kW and  $D^*=1.38$  m

### 2.4.1 Temperature prediction

Figures 17 through 19 give respectively, the time-temperature profile predictions for thermocouples N° 2, 12 and 17. These figures illustrate that the increase of the temperature is not very significant when the fire is well resolved ( $R^*=0.07$ ). Therefore Case 3 will be adopted for this fire.

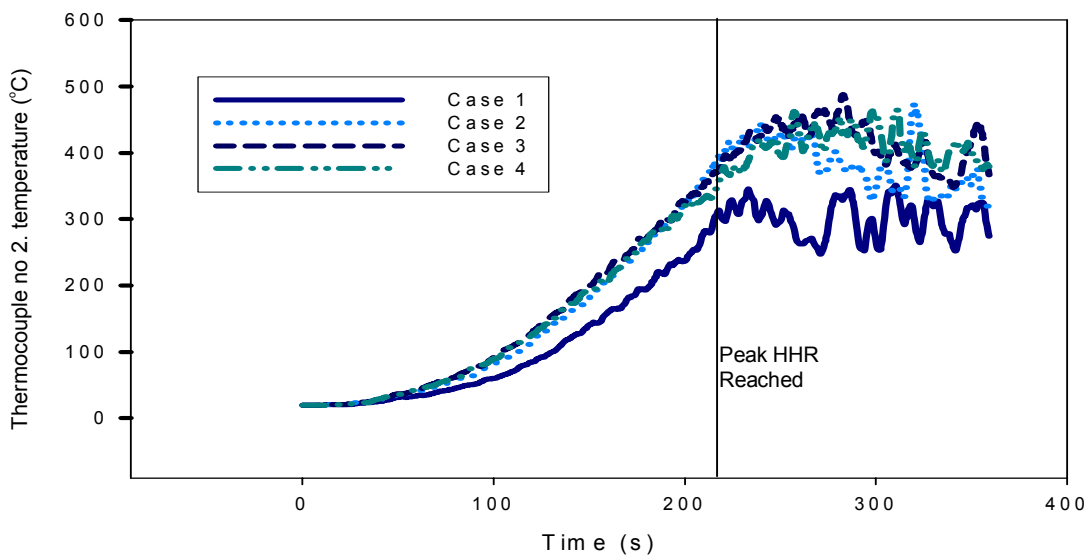


Figure 17: Time-temperature profiles 0.1 m below basement ceiling- SWQP

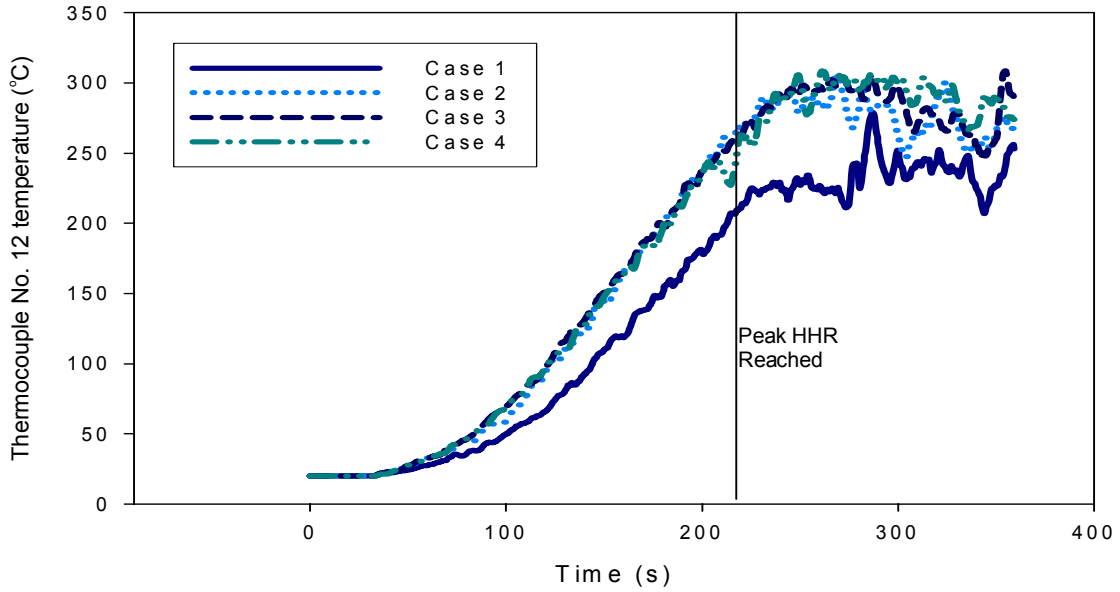


Figure 18: Time-temperature profiles 0.1 m below basement ceiling - NWQP

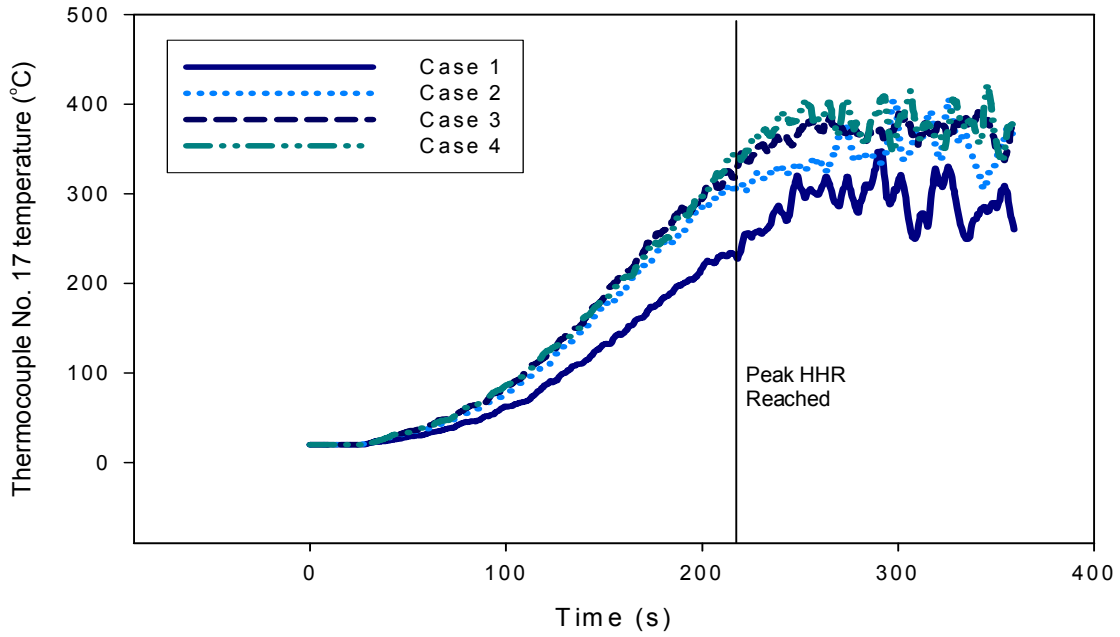
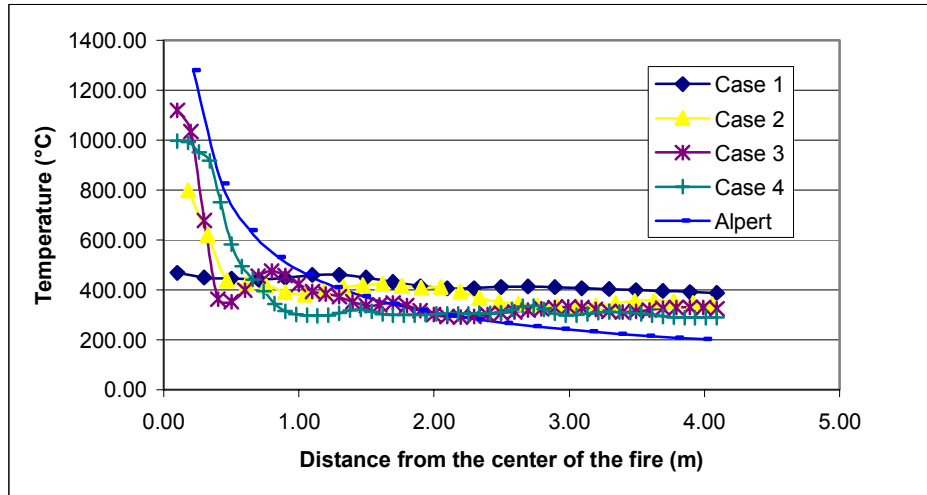


Figure 19: Time-temperature profiles 0.1 m below basement ceiling – NEQP

Figure 20 shows the comparison of the predicted temperature at 0.3 m below the basement ceiling with the Alpert correlation. The Alpert correlation provides an estimation that is closer to Cases 2, 3 and 4 of FDS predictions. The smaller grids provide a better prediction (Fire resolution index close to 1 in Table 14). However a coarse grid provides an average temperature.



**Figure 20: Comparison of FDS Predictions of ceiling jet temperature with Alpert correlation**

### 2.4.2 CO prediction

Figures 21 through 23 give respectively the time-CO concentration profile predictions for measurements N° 43, 45 and 46. The figures show that the effect of the grid is minimal on the prediction of the CO concentrations. The figures show similar trend. The maximum CO concentration observed at this height is approximately 200 ppm which is below to the critical tenability limit criteria adopted, by the Fire Engineering Design Guide<sup>5</sup>, that lead to incapacitation.

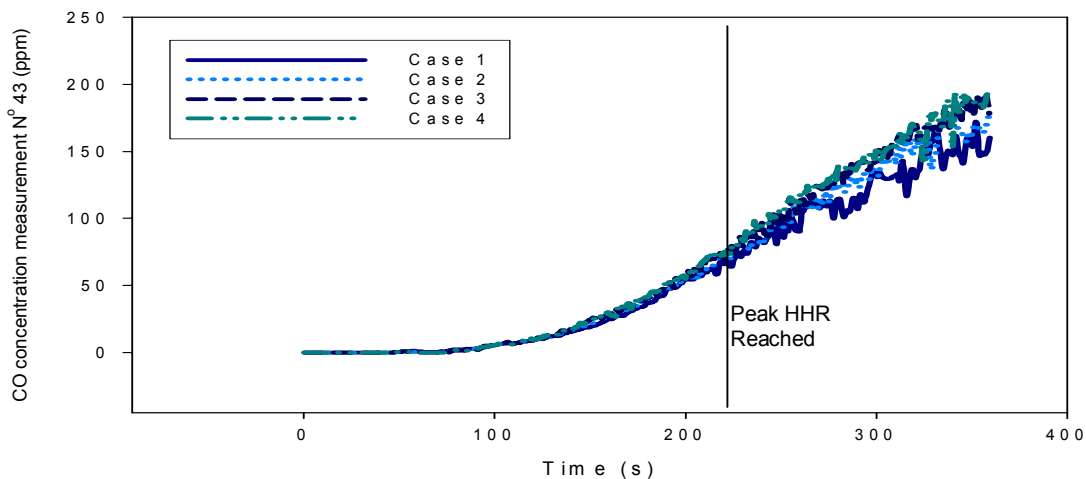


**Figure 21: CO concentration at height 1.5 m- SWQP**

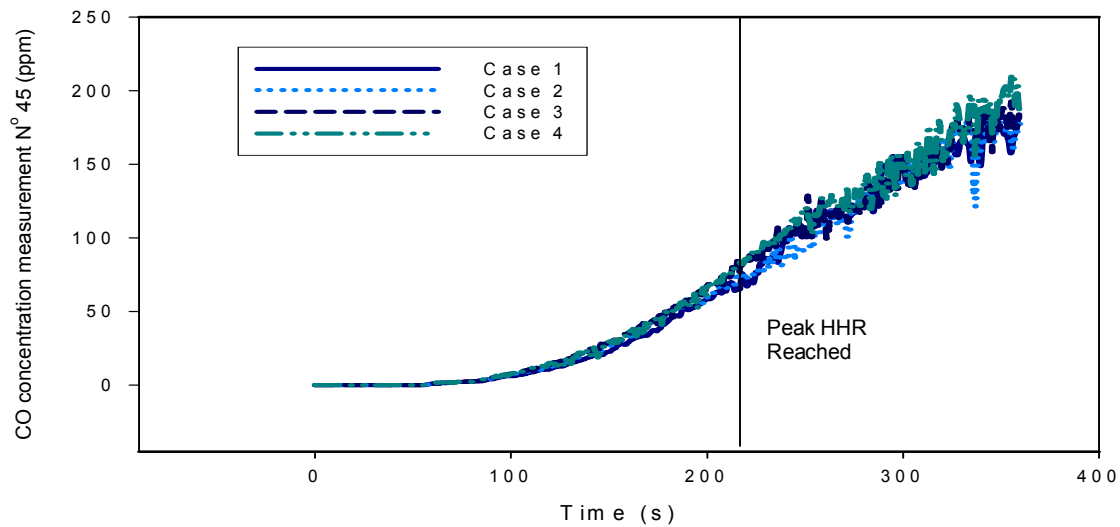


**Figure 22: CO concentration at height 1.5 m - NWQP**

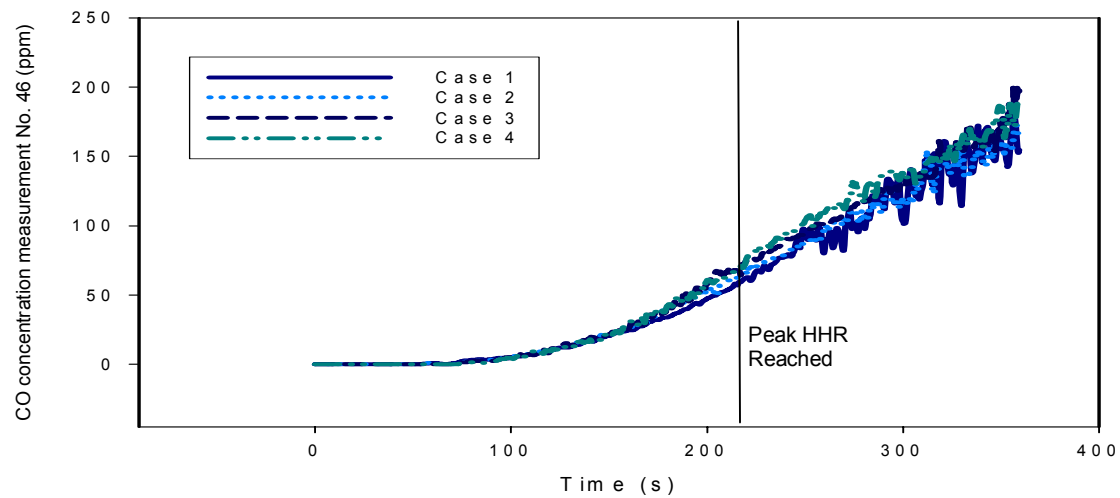


**Figure 23: CO concentration at height 1.5 m - NEQP**

### 2.4.3 CO<sub>2</sub> prediction

Figures 24 through give respectively, the time-CO<sub>2</sub> concentration profile predictions for measurements N° 47, 49 and 50. The figures show that the effect of the grid is minimal on the prediction of the CO<sub>2</sub> concentration. The situation in the basement becomes hazardous at 280 s into the simulation. The CO<sub>2</sub> concentration reaches the tenability limit at 0.05 s mol/mol.

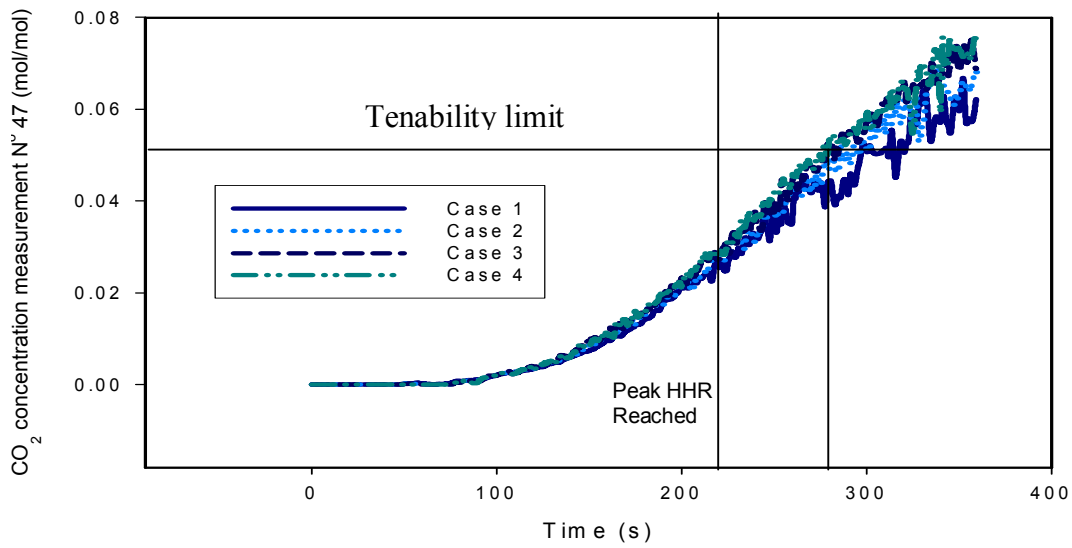


**Figure 24: CO2 concentration at height 1.5 m - SWQP**

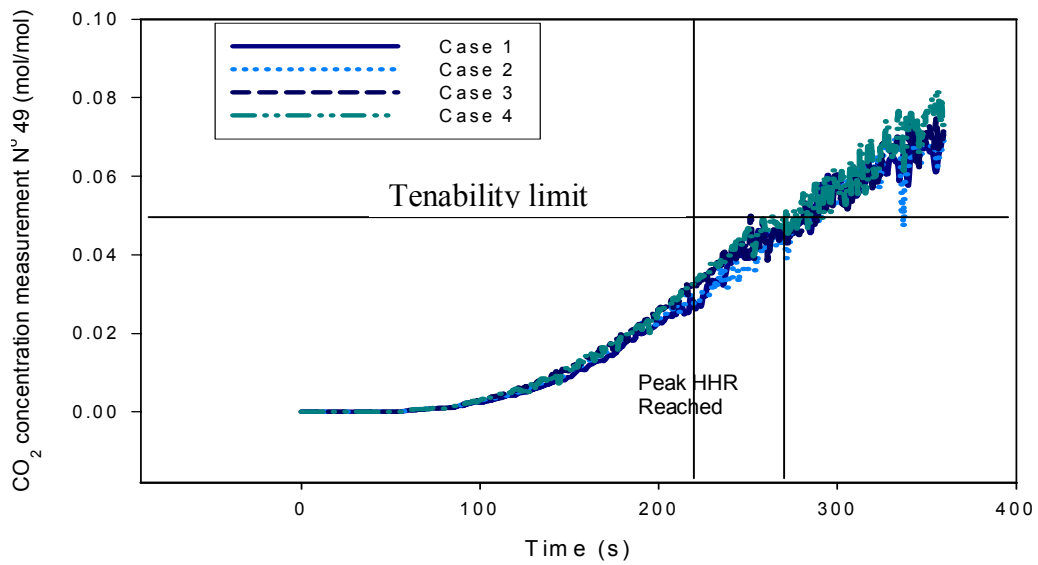


**Figure 25: CO2 concentration at height 1.5 m - NWQP**

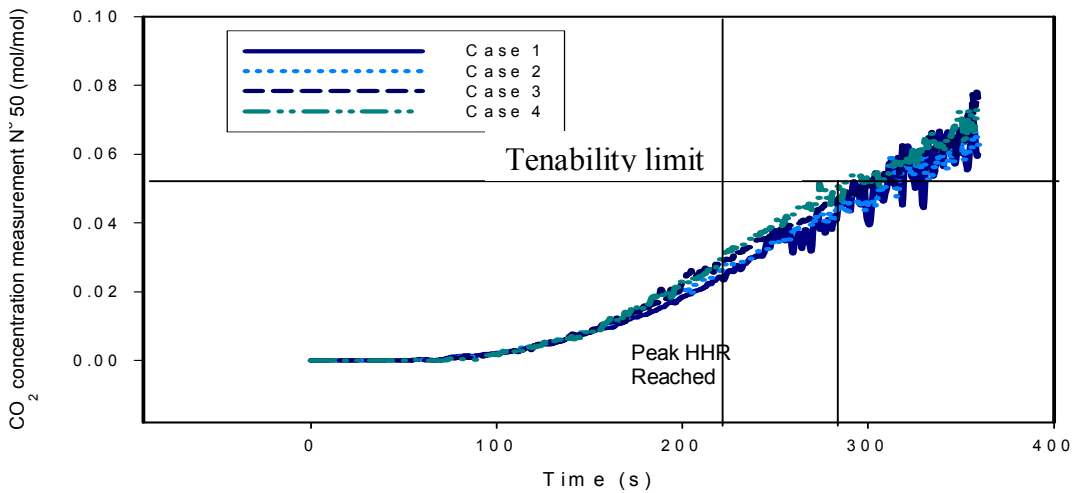


**Figure 26: CO2 concentration at height 1.5 m - NEQP**

#### 2.4.4 Extinction coefficient prediction

Figures 27 through 29 give respectively, the time extinction profile predictions for measurements N° 51 to 54. The figures show that the effect of the grid is minimal on the prediction of the extinction coefficient. The coefficient extinction reaches the tenability limit of  $0.5 \text{ m}^{-1}$  at 180 s, some 70 seconds before the fire released its peak heat releases rate.

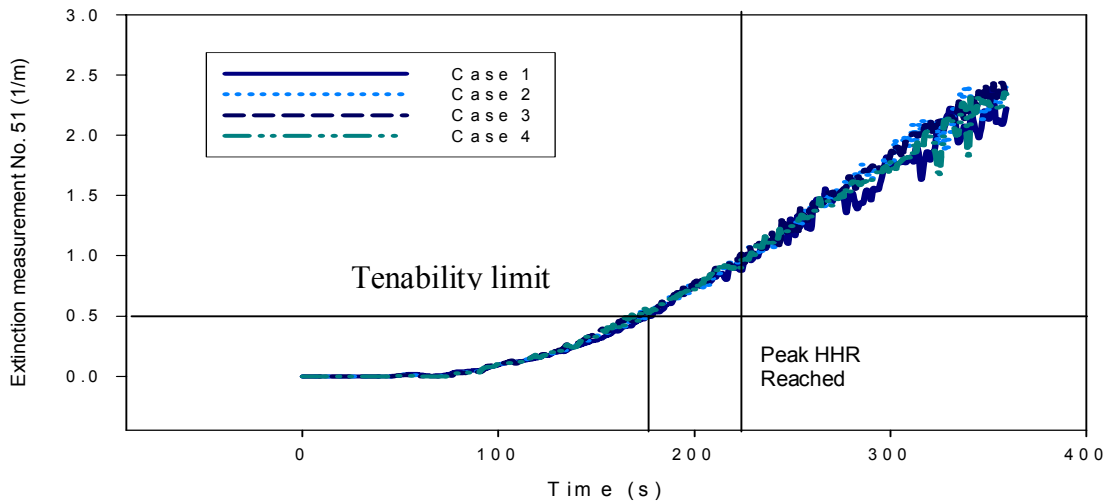


**Figure 27: Extinction coefficient at height 1.5 m - SWQP**

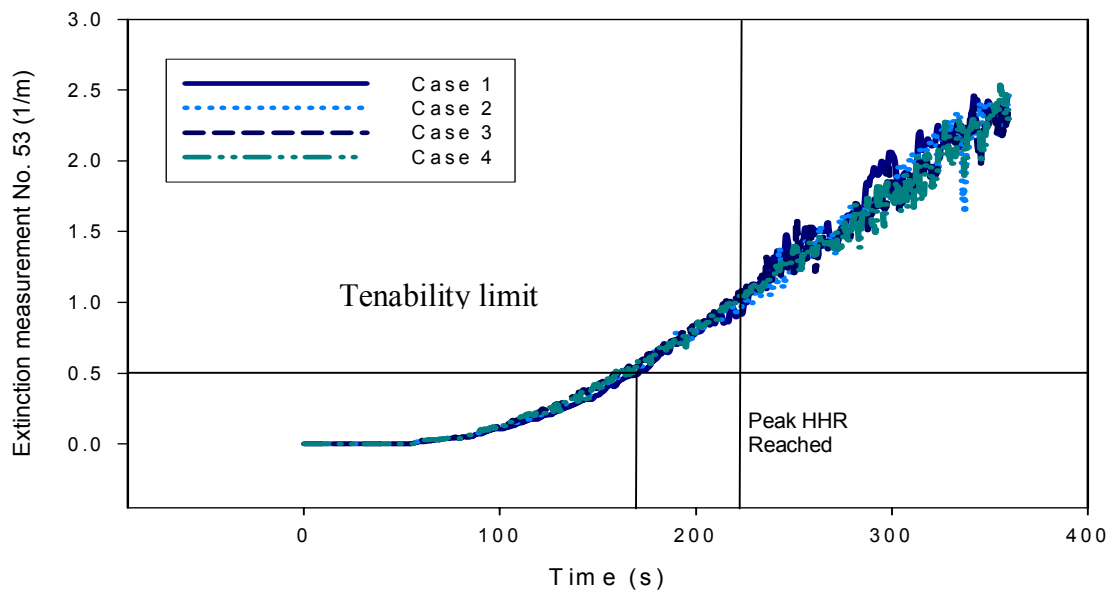


**Figure 28: Extinction coefficient at height 1.5 m - NWQP**

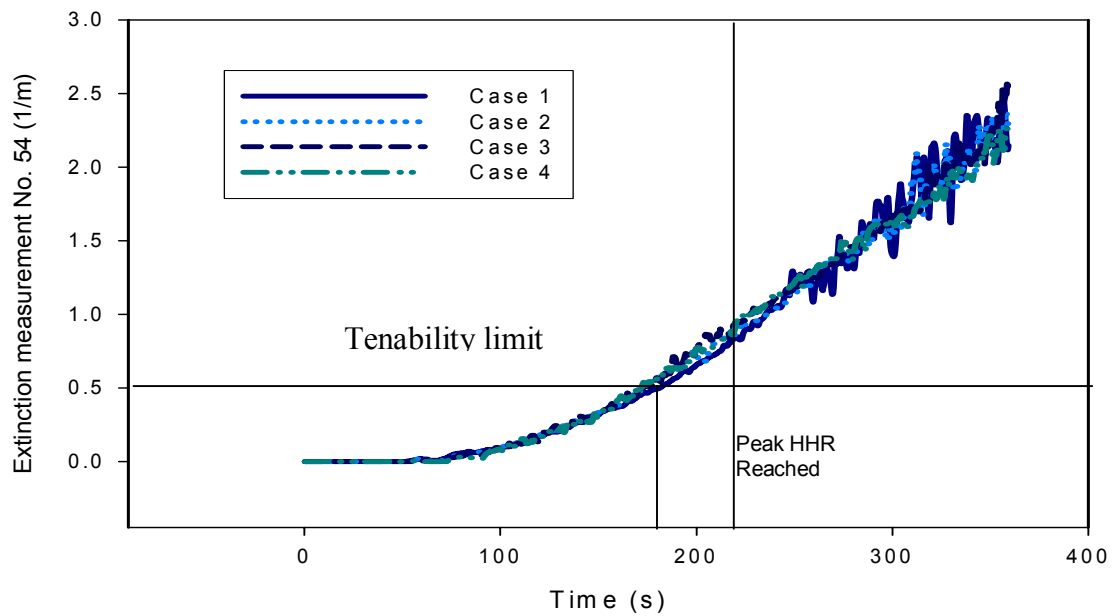


**Figure 29: Extinction coefficient at height 1.5 m N° 54- NEQP**



## 2.5 Fire 3- 3000 kW

The heat release rate of the fire was assumed to follow a fast T-squared fire, reaching a peak of approximately 3 MW in 253 s. The characteristic fire diameter is 1.49 m.

Table 15 summarizes some results from the simulations. The FRI was found to be equal to 1 from the resolution index of 0.07. Thus, the finer grid provides a better prediction. Case 3 was chosen for this fire.

Cases	Grid number	Grid size (cm)	R*	Fire Resolution index	Run time (h)
Case 1	54x45x40	20	0.13	0.84	2.89
Case 2	75x65x20	14	0.09	0.98	8.78
Case 3	108x90x27	10	0.07	1	28.69
Case 4	135x120x36	8	0.05	1	82.31

**Table 15: Fire 3:  $\dot{Q}=3000$  kW and  $D^*=1.49$  m**

### 2.5.1 Temperature prediction

Figures 30 through 32 give respectively, the time temperature profile predictions for thermocouples N° 2, 12 and 17. These figures illustrate that the increase of the temperature is not very significant when the fire is well resolved ( $R^*=0.07$ ). The fire dynamic is well simulated, with a finer grid which catches most important phenomena. As shown in Figure 30 to Figure 32, after the 280 s of the simulation, the temperature starts to decrease due partly to the depletion of available oxygen.

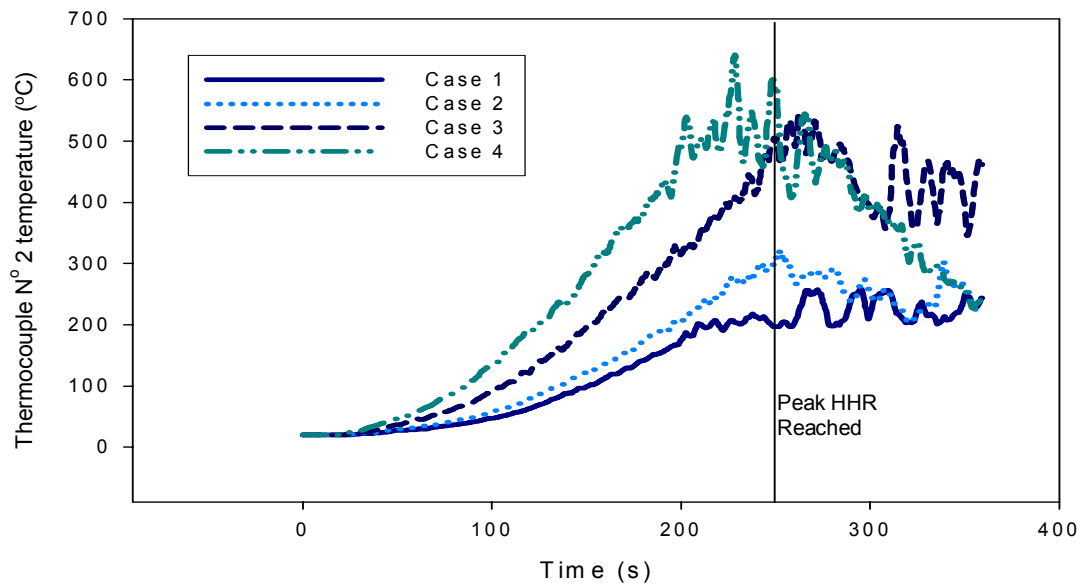


**Figure 30: Time- temperature profiles for thermocouple N° 2- SWQP**

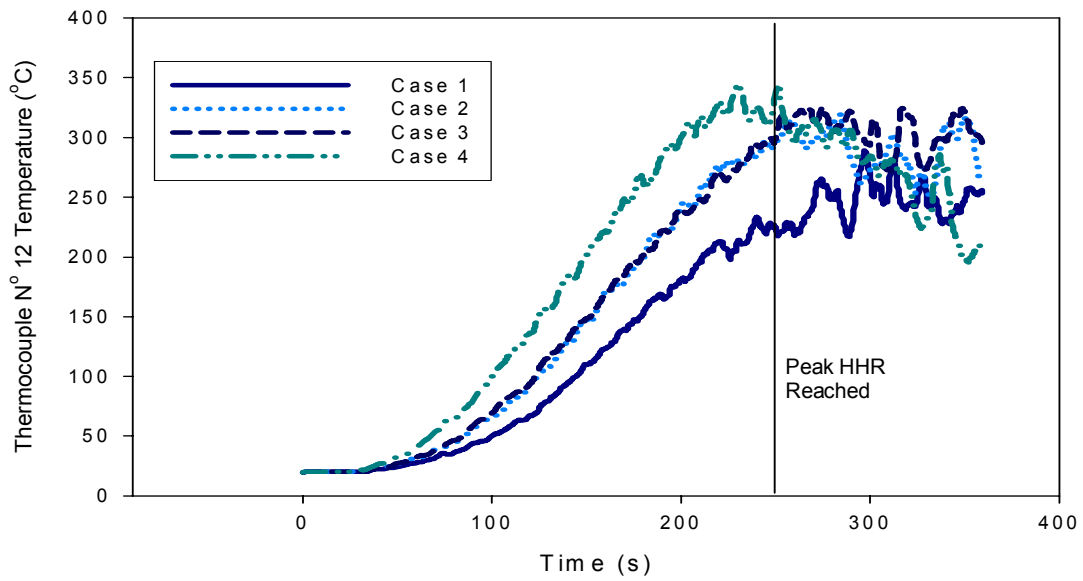


**Figure 31: Time-temperature profiles for thermocouple N° 12- NWQP**

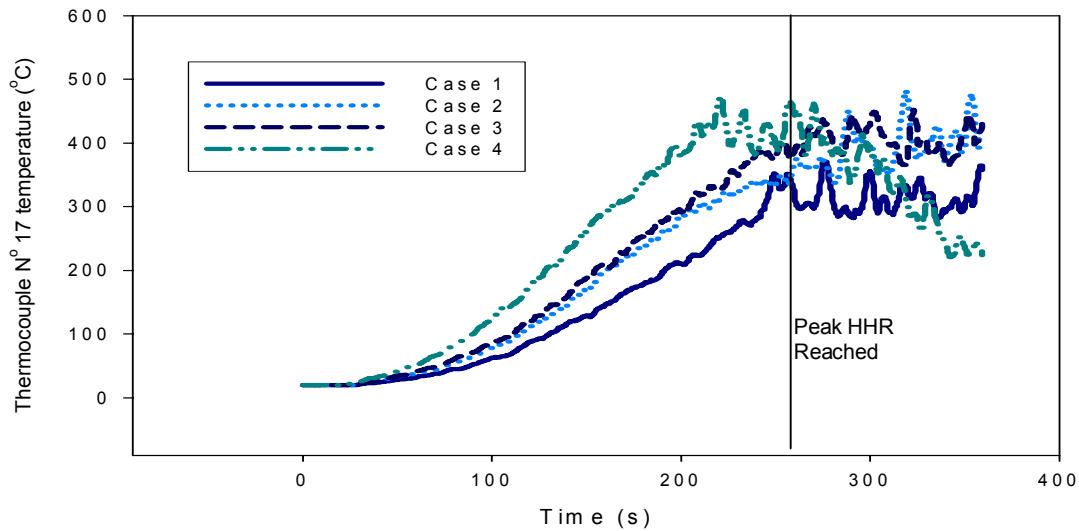


**Figure 32: Time- temperature profiles for thermocouple N° 17- NEQP**

Figure 33 shows the comparison of the predicted temperature at 0.3 m below the basement ceiling with the Alpert correlation. The Alpert correlation provides an estimation that is closer to Cases 2, 3 and 4 of the FDS predictions. The smaller grids provide a better prediction (Fire resolution index close to 1 in Table 15). The coarse grid seems to provide an average temperature.

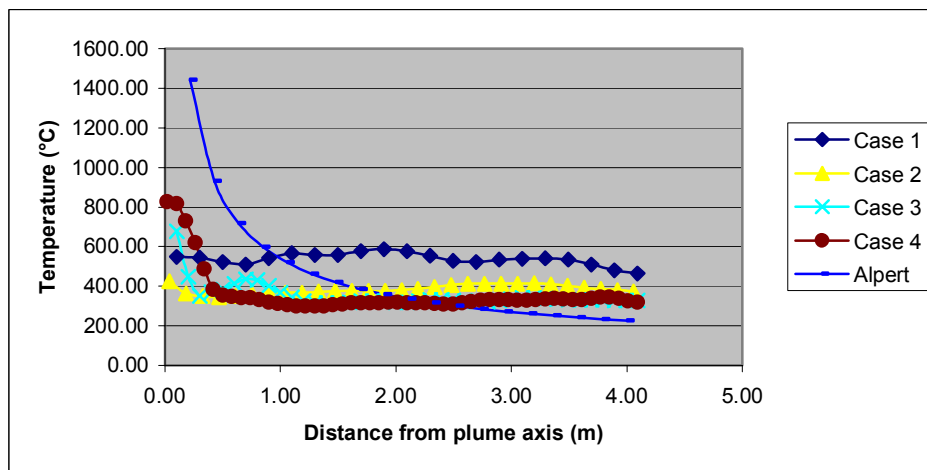


**Figure 33: Comparisons of FDS prediction of the ceiling jet temperature with Alpert correlation**

## 2.5.2 CO prediction

Figure 34 gives the time-CO concentration profile predictions for measurements N° 43, 45 and 46 placed at a height of 1.5 m in three quarter points. The figure shows that the CO concentration is higher with the finer grid. The maximum CO concentration observed at this height is approximately 250 ppm which is below the critical tenability limit criteria adopted by the Fire Engineering Design Guide<sup>5</sup> that leads to incapacitation.

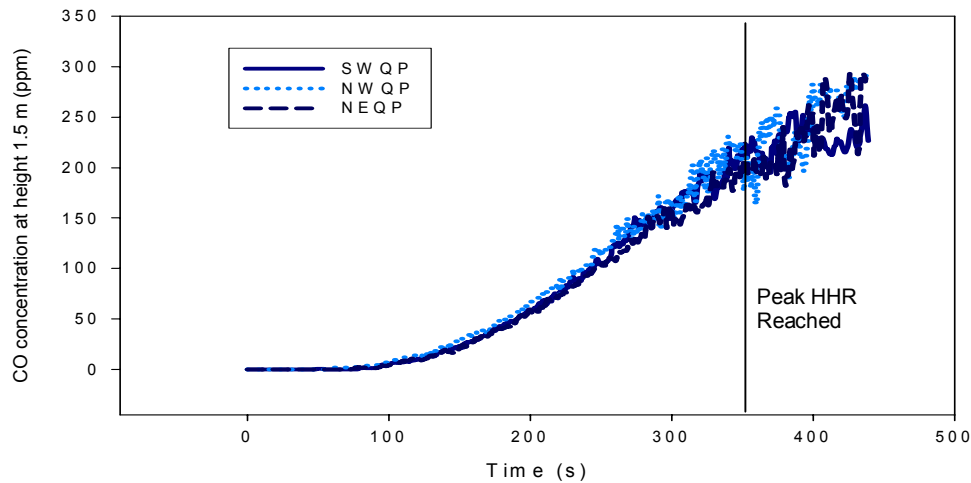
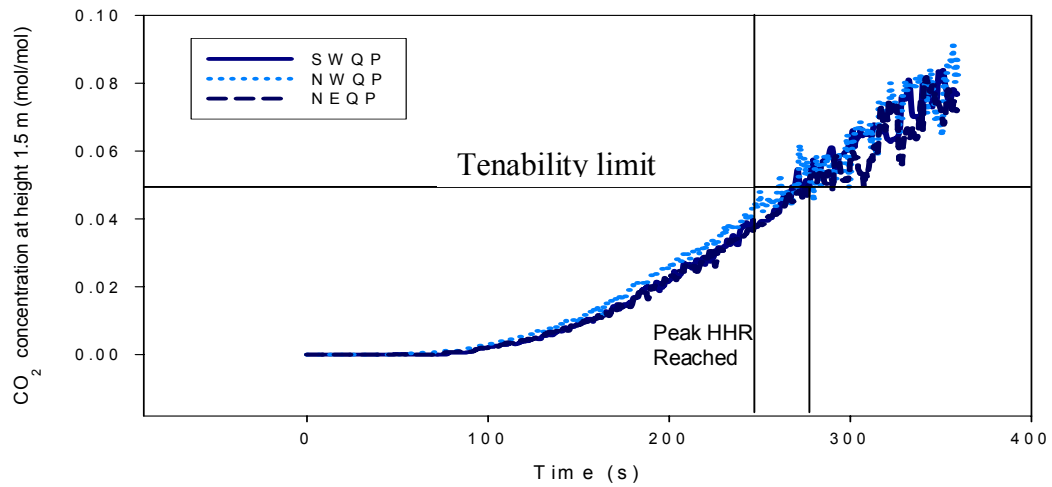


Figure 34: CO concentration at three points of the basement at height 1.5 m

## 2.5.3 CO<sub>2</sub> prediction

Figure 35 gives the CO<sub>2</sub> concentration vs. time for measurements N° 47, 48, 49 and 50 placed at a height of 1.5 m in three quarter points. The figure shows that the situation in the basement becomes very hazardous after 280 s of the simulation when the CO<sub>2</sub> concentration reaches the tenability limit.



**Figure 35: CO<sub>2</sub> concentration at three points of the basement at height 1.5 m**

#### 2.5.4 Extinction coefficient prediction

Figure 36 gives the time-extinction profile predictions for the measurements N<sup>o</sup> 51, 53 and 54 placed at height of 1.5 m in three quarter points. The figure shows that the tenability limit is reached at 180s. Thus, the visibility becomes poor which will delay the escape time of the occupants.

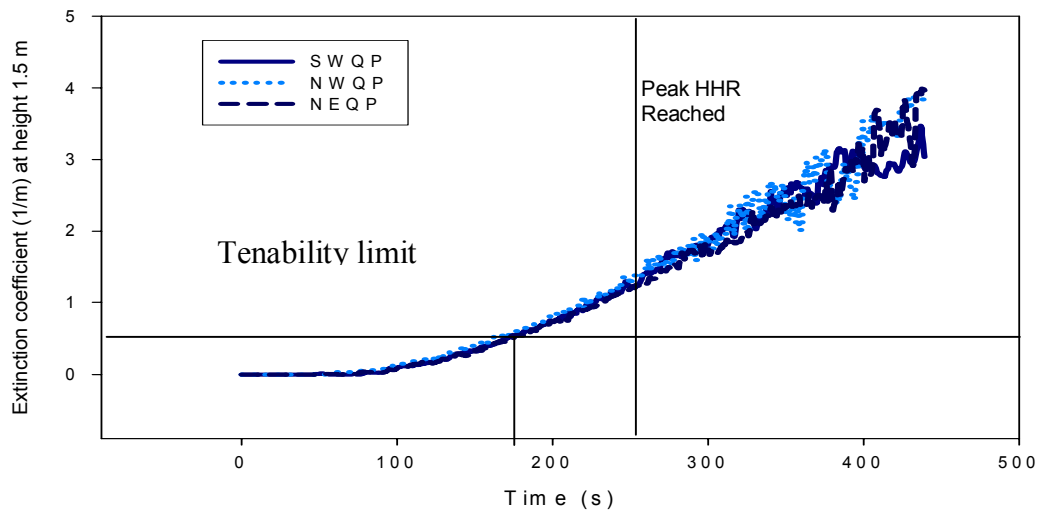


**Figure 36: Extinction coefficient at three points of the basement at height 1.5 m**

## Conclusion

This report presented the details of the grid resolution analysis study for the fire performance of houses undertaken, in order to determine an optimal grid size that will be used to evaluate the fire safety in houses.

CFD simulations were conducted for three different fire sizes and four grid sizes. The numerical simulations showed that the computation time is significantly influenced by the grid sizes specified by the user. As well a finer grid provides a better prediction of the temperature, visibility, CO and CO<sub>2</sub> concentration. A coarse grid gave the worse predictions when compared to correlations. It was observed for the three fire sizes, the Fire resolution index is equal to 1 when the resolution parameter is 0.07. Thus, this value may be used as an indication of an optimum grid size for future simulations.

Based on the critical tenability limit criteria adopted by the Fire Engineering Design Guide<sup>5</sup>, the simulation results predicted that untenable conditions for CO<sub>2</sub> were reached after 280 s for fires 2 and fire 3. The untenable conditions for the visibility criteria were reached after 180 s for fire 1.

## References

1. McGrattan, Kevin B., Baum, Howard R., Rehm, Ronald G., Hamins, Anthony, Forney, Glenn P., Fire Dynamics Simulator – *Technical Reference Guide*, National Institute of Standards and Technology, Gaithersburg, MD., NISTIR 6467, January 2000.
2. McGrattan, Kevin B., Forney, Glenn P., Fire Dynamics Simulator – User’s Manual, National Institute of Standards and Technology, Gaithersburg, MD., NISTIR 6469, January 2000.
3. SFPE Handbook of Fire Protection Engineering
4. T. G. Ma, J. G. Quintiere, Numerical simulation of axi-symmetric fire plumes : accuracy and limitations , *Fire Safety Journal* 38, 467-492, 2003.
5. A. H. Buchanan, Fire Engineering Design Guide, *Center for Advanced Engineering, University of Canterbury, New Zealand, 1994.*
6. P. Feng, G. V. Hadjisophocleous and D. A. Torvi, “ Equations and Theory of the Simple Correlation Model of FIERAsystem”, *Internal Report N° 779, Institute for Research in Construction IRC, February 2000.*
7. Heskestad, G., “Fire Plumes”, Chapter 2-2, *SPE Handbook of Fire Protection Engineering, Society of Fire Protection Engineers, Quincy, MA, USA, 1995.*
8. Alpert, R. L. and Ward, E. J., “Evaluating Unsprinklered Fire Hazards”, *SFPE Technology Report 83-2, Society of Fire Protection Engineers, Boston, MA, 1983.*
9. SPE Handbook of Fire Protection Engineering, Third Edition, 2002.